Energy dissipation and multifragment decay in the ^{3}He+^{nat}Ag system

K. Kwiatkowski,[1] W. A. Friedman,[2] L. W. Woo,[1] V. E. Viola,[1] E. C. Pollacco,[3]
C. Volant,[3] and S. J. Yennello[4]
[1]*Department of Chemistry and Indiana University Cyclotron Facility, Indiana University, Bloomington, Indiana 47405*
[2]*Department of Physics, University of Wisconsin, Madison, Wisconsin 53706*
[3]*DAPNIA-Service de Physique Nucléaire, Centre d'Etudes Nucléaires de Saclay, F-91191 Gif-sur-Yvette, Cedex, France*
[4]*Department of Chemistry, Texas A&M University, College Station, Texas 77843*
(Received 17 June 1993)

Multifragment emission data from the ^{3}He+Ag reaction are examined in the context of an intranuclear cascade code followed by an expanding, emitting source calculation. The role of Δ resonances in the energy dissipation process is stressed. In addition, the importance of employing a distribution of excitation energies in such analyses is pointed out. In order to describe the data within the context of this hybrid model, excitation via Δ resonance formation and expansion of the emitting source are required.

PACS number(s): 25.70.Pq, 25.40.Ve, 25.55.−e

I. INTRODUCTION

When two nuclei collide at high enough energy, there is a high probability that the central collisions will lead to a final state with several complex nuclear fragments of intermediate mass (IMFs). This process has been called multifragmentation. To describe such a process completely, one would, in principle, be required to trace the evolution of the entire many-body system from the initial excitation, by means of the nucleon-nucleon interactions, all the way to the emission of both nucleons and complex fragments. A rigorous description appears to be beyond the capabilities of current theory. Nonetheless, important progress toward a reasonably full description, which involves both microscopic and macroscopic aspects of the process, has been made during the past few years [1–6]. The extensive multifragmentation data sets that are now emerging from various detector arrays [6–9] are serving to challenge and stimulate further theoretical advances toward even more complete description and consequent understanding.

The complexity associated with reactions at intermediate energies is well illustrated by the results of linear momentum transfer and mass-yield measurements carried out during the past decade [10–12]. These studies have demonstrated that the initial target-projectile interaction in such collisions generates a broad distribution of residual nuclei and excitation energies. For an understanding of multifragmentation, it is therefore essential to obtain these distributions through realistic treatment of the impact geometry, pre-equilibrium emission, and excitation mechanisms. For light-ion-induced reactions well above the Fermi energy, the intranuclear cascade code [13,14] can be used to evaluate these features, which are related to the initial energy dissipation. For heavy ions, however, the evolution of the mean field of the colliding nuclear system also significantly influences the reaction dynamics, and more elaborate BUU approaches are required [15–17]. For both light and heavy projectile, the important question arises as to the time at which equilibrium (if any) is achieved, and how to couple to the subsequent decay stage self-consistently.

At present, the treatment of the later decay of excited residues must be joined to some appropriate dissipation model. Numerous theoretical approaches have been proposed for this decay stage [1,18–25]. These span two broad classes of calculations: (1) statistical models, in which rate-dependent phenomena govern the distribution of final states, and (2) microcanonical models, for which the predictions depend primarily on the initial, time-independent, state of the system. Compression and expansion of nuclear matter, as well as the fluctuations due to initial N-N two-body interactions, are of major concern in these approaches. One of the primary goals sought in the study of the various multifragmentation decay models is an understanding of the nuclear equation of state at low density. Attempts to obtain such information from fits to experimental data are highly uncertain, however, without accurate accounting of the energy dissipation stage of the reaction.

In the analysis presented here, we focus on multifragment events produced in light-ion-induced reactions. Light-ion projectiles provide several important advantages for the study of multifragmentation, among them: (1) isolation of a single emitting target-like source, free of contributions from projectile decay or "fireball-like" sources; (2) small kinematic distortions of the ejectile spectra, due to the low center-of-mass velocity of the emitting source; (3) easily identifiable forward-angle yields; (4) low angular momentum, and (5) minimal collective effects, i.e., compression and initial source expansion velocity are small. The last point is particularly relevant in the sense that light-ion studies form an important baseline for deducing such effects in heavy-ion-induced reactions.

Much of the early interest in the emission of intermediate mass fragments (IMFs) was stimulated by studies of proton-induced reactions [26]. More recently, inclusive studies of the ^{3}He+^{nat}Ag system at energies up to

3.6 GeV have suggested a change in mechanism at bombarding energies in the vicinity of 1.8 GeV total energy [27]. Subsequent coincidence studies [8] with ^{3}He beams have demonstrated the existence of multifragmentation events for this system. In the present work we examine these latter results in the context of a model in which the energy dissipation stage is described by the intranuclear cascade code (INC) [13] and the decay is described by an expanding, emitting source (EES) undergoing statistical decay [1]. The EES model has previously been successfully employed in the interpretation of the fragment-emission temperatures deduced from the relative population of states. It has also been used to gain general insight into the multifragmentation mechanism and to describe IMF multiplicity yields and kinematic features in specific heavy-ion-induced reactions [6]. The predictions of these combined models are compared with the coincidence data for 3.6 GeV ^{3}He ions incident on an Ag target [8,27].

II. ENERGY DISSIPATION: THE ROLE OF THE Δ (3,3) RESONANCE

In the case of light-ion-induced reactions, it is especially important to treat the initial energy dissipation stage carefully since there are a relatively small number of N-N collisions, and there is substantial transparency for the incoming particles. These two effects conspire to generate an exponentially falling excitation energy, E^*, distribution that extends over a very wide range [28].

As discussed in the introduction, the intranuclear cascade code [13,14] has proved successful in describing the energy dissipation process in light-ion-induced reactions on medium-to-heavy target nuclei. In this section we report on an investigation of the energy dissipation in the ^{3}He+^{nat}Ag reaction, using the Weizmann Institute version of the intranuclear cascade code ISABEL [13]. We have paid particular attention to the role that excitation of the Δ resonance plays in producing large excitation energies on a very fast time scale (~20 fm/c). This emphasis is motivated by two features of the experimental data. First, as we have already noted, there is a change in reaction observables for the ^{3}He+^{nat}Ag system [27] between 0.90 and 1.8 GeV (E/A = 300–600 MeV). This corresponds to N-N collision energies near the peak of the Δ resonance excitation function. Second, calculations show that Δ formation followed by rescattering and/or isotropic decay with reabsorption of the pion provides a rapid, efficient mechanism for depositing large excitation energies and transverse momenta in the struck nucleus [29]. This feature offsets the low probability for density compression in light-ion-induced reactions.

The ISABEL intranuclear cascade calculations were performed using options in the code which emphasize the formation of highly excited residual nuclei—a condition necessary to enhance the probability for multifragmentation. The salient code options are summarized in Table I. Most important among these is the inclusion of fast rearrangement during the cascade. This assumption has been shown to reproduce experimental data for central collisions in heavy-ion-induced reactions at similar projectile E/A values, and at the same time account for fast nucleon spectra and multiplicities [13]. Cascade-cascade interactions have also been permitted, an effect which has been shown to increase pion absorption, especially in heavy-ion collisions [30]. In principle, one could further enrich the calculated spectrum of high excitation-energy events by modifying the input-scattering cross sections. However, this would require assumptions about unknown in-medium effects, which we do not attempt to address.

In Fig. 1 the average excitation energy predicted by the ISABEL code for the ^{3}He+^{nat}Ag system is shown for incident energies below 4 GeV. The curves show the average excitation energy for three impact parameter, b, regimes: central collisions ($b < 2.6$ fm), intermediate impact parameters ($2.6 \leq b \leq 4.4$ fm), and more peripheral interactions ($b > 4.4$ fm). Assuming a radius parameter of $r_0 \cong 1.4$ fm, these values correspond to approximately 10%, 20%, and 70% of the total reaction cross section, respectively. It is observed that for events with the largest impact parameters, i.e., most of the cross section, the average excitation $\langle E^* \rangle$, remains relatively low and insensitive to bombarding energy, $E_{\rm beam}$, with $\Delta\langle E^* \rangle / \Delta E_{\rm beam} \approx 25$ MeV/GeV. In the intermediate impact parameter region, the average excitation energy increases more rapidly, $\Delta\langle E^* \rangle / \Delta E_{\rm beam} \approx 85$ MeV/GeV, reaching values near 400 MeV at 4 GeV bombarding energy. For the most central collisions the average excitation energy grows even more rapidly, $\Delta\langle E^* \rangle / \Delta E_{\rm beam} \approx$ 130 MeV/GeV, with $\langle E^* \rangle$ values well in excess of the predicted multifragmentation threshold [1,18]. It is in this impact parameter region that the excitation of Δ resonances is predicted to be most probable [29]. For all impact parameters the widths of the distributions in E^* grow monotonically with increasing bombarding energy.

TABLE I. Input for ISABEL INC calculation [13].

Total density is reduced after each collision; fast rearrangement option
Cascade-cascade interactions allowed; maximum distance=3.0 fm
Standard step size=0.6 fm
Isobar included with no refraction or reflection
Isobar nucleon exchange allowed
Energy-dependent isobar resonance width [G. Ginnocchio, Phys. Rev. C **17**, 195 (1978)].
Distance restriction=1.10 fm; isospin dependent
Projectile is Lorentz-contracted
Eight density regions employed; Thomas-Fermi local density approximation for momenta
Other parameters: default values

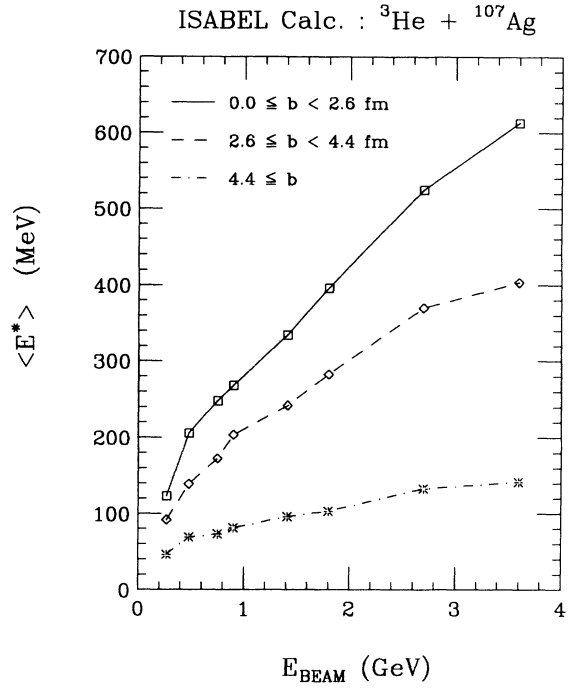

FIG. 1. Predictions of ISABEL code[13] for average excitation energy as a function of bombarding energy for the ^{3}He+^{nat}Ag system. Results are shown for three impact parameter regimes as indicated in figure.

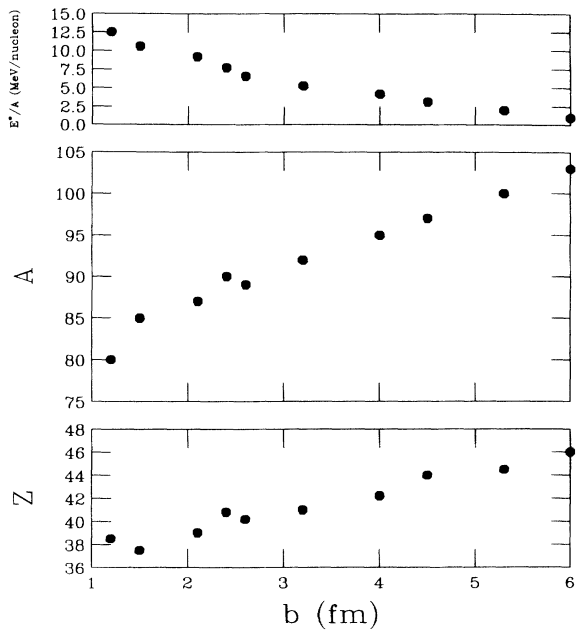

FIG. 2. Upper frame: Average excitation energy per residue nucleon number A as a function of impact parameter b for 3.6 GeV ^{3}He+^{nat}Ag reaction. Middle and lower frames, respectively; average residue mass A and charge Z as a function of impact parameter for above reaction.

Another important feature observed in these calculations is the relationship between excitation energy and the mass and charge loss in the cascade. Figure 2 shows predictions for the average mass, charge, and excitation energy per nucleon of the residual nuclei formed at 3.6 GeV incident energy as a function of impact parameter. Values of $E^*/A \approx$10–12 MeV are predicted for the most central collisions with a monotonic decrease for increasingly peripheral reactions. Figure 2 also shows that for collisions with small impact-parameters, considerable mass and charge loss occurs in the collision stage (up to 30 nucleons) and that this loss is correlated with very highly excited residues. This correlation can be characterized by $\Delta\langle E^*\rangle/\Delta A \approx 33$ MeV nucleon, where ΔA is the mass lost. These correlations suggest that both neutron and proton multiplicities provide a gauge of the impact parameter in these collisions, especially when they include the mass lost due to subsequent evaporation.

Figure 3 shows the excitation energy distribution for the 3.6 GeV+^{nat}Ag system for collisions which deposit excitation energies greater than $E^* \geq 50$ MeV. The dashed curve gives the predictions of the ISABEL code, which includes cross sections for Δ resonance formation, decay, and pion reabsorption. For comparison, the solid curve provides the distribution in excitation energy when the inelastic cross sections for Δ production in ISABEL have been suppressed by a factor of 10. This should reveal the excitation energy distribution that would arise primarily due to N-N elastic scattering. The effect of the Δ resonance in enhancing high excitation energy events is apparent. The standard form of ISABEL, with Δ's, predicts that for these events with $E^* > 50$ MeV, about 33% will produce residues with excitation energies greater than 500 MeV. With the N-N inelastic channels suppressed, only 12% of the probability distribution exceeds 500 MeV. In Fig. 4 we compare the relative probability for depositing more than 500 MeV of excitation energy as a function of bombarding energy for two sets

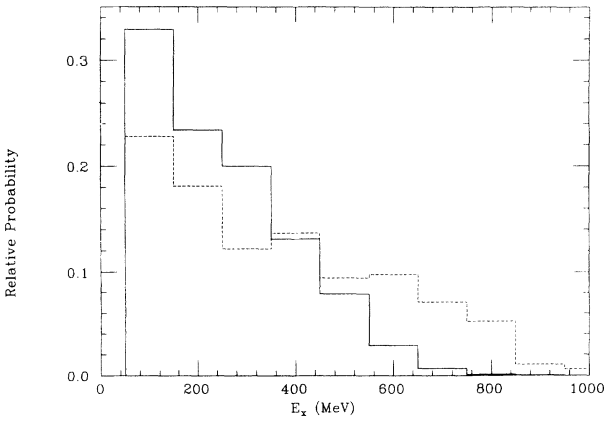

FIG. 3. Distribution of excitation energies for residues with $E^* > 50$ MeV predicted by the ISABEL code[13] for the 3.6 GeV ^{3}He+^{nat}Ag reaction. Calculations are averaged over 100 MeV bins. Dashed curve is for standard ISABEL code with fast rearrangement. Solid line is same calculation with cross sections for Δ production reduced by a factor of 10.

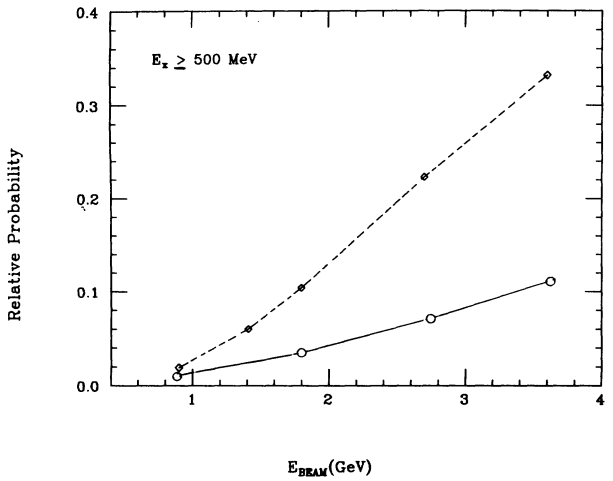

FIG. 4. INC predictions of the probability for exciting residues to energies greater than 500 MeV as a function of beam energy for the ^{3}He+^{nat}Ag reaction. Dashed line is for standard ISABEL; solid line is for the case of no Δs.

of calculations, one with Δs and one with the Δ suppressed. The importance of the Δ resonance for incident energies above about 1 GeV is apparent. This sensitivity suggests that multifragmentation studies with light-ion probes is strongly influenced by Δ formation and pion reabsorption.

The INC code makes another important prediction; this one with respect to the reaction dynamics. It concerns longitudinal and transverse momentum transfers, $p_{\|}$ and $p_{\perp}$. Figure 5 shows the average values of these

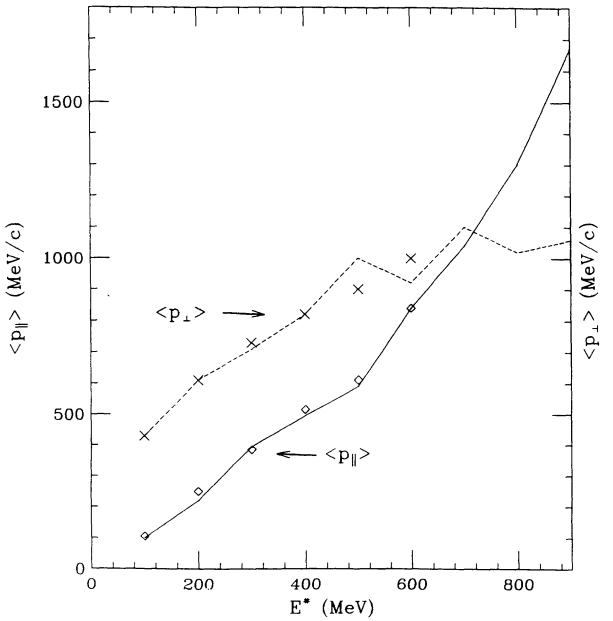

FIG. 5. ISABEL prediction of average longitudinal momentum transfer (left) and perpendicular momentum transfer (right) associated with a given residue excitation energy. Standard ISABEL (Δ) is shown by solid line for $\langle p_{\|} \rangle$ and dashed line for $\langle p_{\perp} \rangle$; case for no Δs is given by ($\diamond$) for $\langle p_{\|} \rangle$ and x for $\langle p_{\perp} \rangle$.

two momentum components as a function of deposited excitation energy for the 3.6 GeV ^{3}He+^{nat}Ag reaction. Calculations were performed for two cases, one with and one without the Δ resonance, as was done to produce the predictions of Figs. 3 and 4. Here one sees that the correlation between the excitation energy and each component of the momentum transfer is quite insensitive to the influence of the Δ resonance, although in the absence of the Δ, the range of $p_{\|}$ and $p_{\perp}$ is limited due to the much lower probability of forming highly excited residues. Figure 5 also shows that for those events with low excitation energy, $\langle p_{\perp} \rangle$ is much larger than $\langle p_{\|} \rangle$. In addition, the distribution in $p_{\perp}$ is very broad. This is consistent with the more peripheral nature of these interactions (see Fig. 1). On the other hand, for residues with excitation energies greater than about 500 MeV, the values of $p_{\|}$ and $p_{\perp}$ reverse roles, with $\langle p_{\|} \rangle$ continuing to grow while $\langle p_{\perp} \rangle$, remains nearly constant.

One of the distinctive features of the multifragment coincidence studies of Yennello *et al.* [8] was the observation, in a rapidity plot, that the velocity of the sources was relatively constant, independent of fragment charge or kinetic energy for events with IMF multiplicity $M \geq 3$. Depending on the assumed mass of the emitting source, this observation suggested an average value of $p_{\|}$ between 1.0 and 1.2 GeV/c. Using this with the correlation indicated in Fig. 5, one deduces an average excitation energy of 600–800 MeV for this set of multifragment events. In this regime, we also observe that $p_{\perp} \approx p_{\|} \approx 1$ GeV/c, a result consistent with the nearly isotropic angular distribution and rapidity plots that are observed for IMFs in the 3.6 GeV ^{3}He+^{nat}Ag reaction.

In summary, the ISABEL code predicts that for the most central collisions, the energy dissipation stage for light-ion induced reactions can produce significant yields of target-like residues well above the fragmentation threshold. The Δ resonance appears to play a crucial role in enhancing excitation energy deposition. Linear and transverse components of the momentum transfer are in good accord with experimental observations for high E^* events. Thus we proceed to the investigation of the multifragment decay stage under the assumption that the reaction dynamics of the initial stage are reasonably well under control.

III. FRAGMENTATION FROM AN EXPANDING, EMITTING SOURCE

Given the mass, charge, and excitation energy distributions of the hot residues following the cascade, as predicted by the INC code, we can now consider the subsequent deexcitation of these residues. In this section, we examine the ^{3}He+^{nat}Ag data in the context of the expanding emitting source model [1]. This schematic model treats the dynamical response of a nuclear system, starting at normal density with a given mass, charge, excitation energy, and radial expansion velocity. It considers monopole expansion driven by the thermal pressure of the system and an effective restoring nuclear force. For the system studied here, the expansion time is of the or-

der of 60–70 fm/c. Statistical decay is permitted during the expansion phase by introducing density-dependent transition rate expressions. This model thus extends the dynamical expansion following the initial excitation phase into the decay phase. In this respect it is important to note two important consequences of the INC dynamics. First, most of the energy dissipation is predicted to occur during the first 20–40 fm/c following the first interaction between target and projectile [29]. This permits a temporal separation of excitation and decay. Second, for small impact parameters the INC suggests a collision-driven nucleon distribution that eventually grows radially as a function of time. Thus, in terms of both time scale and the nuclear matter distribution, the INC and EES models contain qualitatively consistent physics.

The EES model predicts both fragment multiplicity distributions and kinetic energy spectra. It is sensitive to the nuclear equation of state at low density through an effective compressibility which relates the binding energy of a finite cold nucleus to the mean density. For simplicity, the relationship is taken as parabolic with a minimum at normal nuclear density, ρ_0, and a value there consistent with liquid-drop binding energies E_{ld}, and with a compressibility K

$$E(\rho)/A = E_{ld}(\rho_0)/A + (K/18)[1 - (\rho/\rho_0)]^2. \quad (1)$$

The model predicts a distinct increase in the mean number of IMFs as E^*/A approaches 8 MeV, an excitation populated with increasing probability for the ^{3}He+^{nat}Ag reaction above about 1 GeV incident energy. The EES calculations performed here were used, in conjunction with the INC predictions, to predict IMF multiplicity distributions and spectra for comparison with the measurements of Yennello *et al.* [8,27]. All the calculations were performed with the assumption that the initial expansion velocity is zero, which, as stated in the introduction, should be a good assumption for light-ion-induced reactions. In addition, the model does not explicitly treat the effect of the angular momentum of the source, using instead level densities that are blind to angular momentum.

The fundamental ingredients of the calculation are a set of calculations at given mass, charge, and excitation energy, with a subsequent convolution of the results of these calculations with weights provided by the ISABEL results. In the calculations for a given excitation energy the source charge and size were taken as the average values of these quantities associated with events in a given bin of excitation energy (100 MeV bin size). To predict the observed multiplicity distribution for IMFs, taken here to be fragments of with $Z \geq 3$, we performed the following sum

$$P(n) = \sum_i \Delta E^* W(i) P(n; E_i^*, A_i, Z_i), \quad (2)$$

where the values of the multiplicity distribution $P(n; E_i^*, A_i, Z_i)$ for a given set of initial conditions (labeled by i) are provided by the EES calculations, and weights $W(i)$ are provided by the INC.

In Fig. 6 we compare the relative multiplicity (M) distribution from the 3.6 GeV data of Ref. [8] with EES calculations for several values of the compressibility parameter K, defined in Eq. (1). Here K was given values of 144, 200, and ∞. All results are normalized to the same value at $M = 2$ to permit comparison. Since the expansion rate decreases as K increases, the $K = \infty$ case corresponds to statistical decay from a compound nucleus at fixed, normal density. For this case the calculation severely underestimates the high multiplicities. Similar comparisons with the GEMINI code [20], which included angular momentum ($l_{max} = 76\hbar$), have also been shown [31] to underpredict the data by nearly 3 orders of magnitude at $M = 4$. These comparisons demonstrate a strong sensitivity of the multiplicity distributions to the compressibility parameter. The best fit seems to be associated with $K = 144$, which is at the lower bound of the range of K found in a similar analysis of heavy-ion reactions [6]. When the $M = 2$ cross section was set to 130 mb, as indicated by the results of Ref. [8], one finds a total reaction cross section of about 2500 mb—which is in qualitative agreement with the expectation for the ^{3}He+Ag. (For touching sphere geometry, this corresponds to an r_0 of about 1.44 fm.) Other values of K, similarly normalized, require much larger values for the total reaction cross section, while providing poorer M distributions.

It is also of interest to examine the sensitivity of the predicted multiplicities to the INC input used for the EES calculations. In Fig. 7 we compare the multiplicity distributions for the 3.6 GeV ^{3}He+^{nat}Ag reaction with INC/EES calculations which include the Δ resonance in one case and suppress it in the other. In both cases the compressibility parameter of $K = 144$ was used, and results displayed are normalized to $M = 2$. The important role of the Δ is apparent. With only N-N elastic scattering in the INC calculations, the combined models

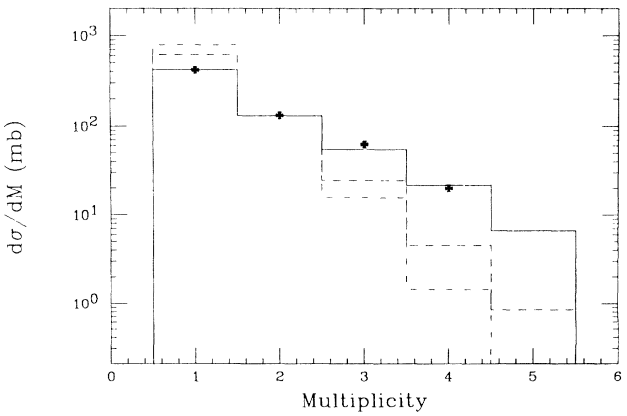

FIG. 6. Multiplicity distribution for 3.6 GeV ^{3}He+^{nat}Ag reaction for several values of the compressibility parameter K, all normalized to the same differential cross section at $M = 2$. Data are given by crosses. INC input to the EES calculation was standard ISABEL. Results for different values of K are $K = 144$ (solid line), $K = 200$ (dashed line) and $K = \infty$ (dot-dashed line).

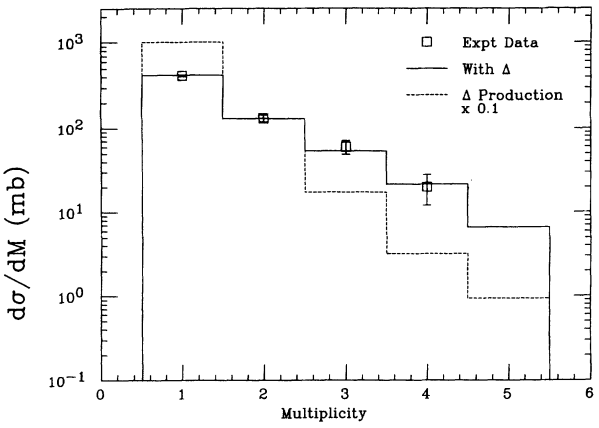

FIG. 7. Multiplicity distribution for EES calculation with $K = 144$ in Fig. 6 (solid line). Dashed line is same comparison, except the INC input does not include Δ production. Data are given by squares.

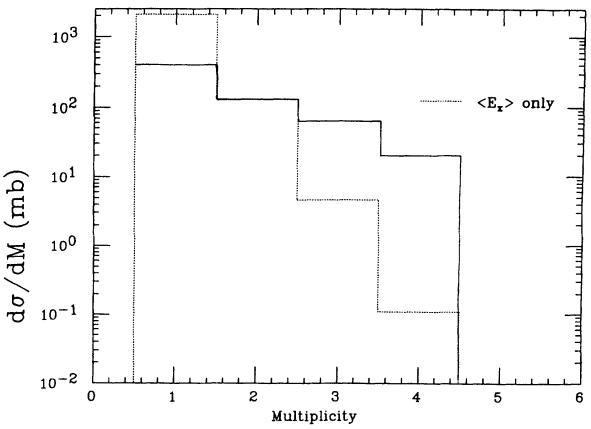

FIG. 8. Multiplicity distribution for EES calculation with $K = 144$ and standard INC calculation, except the average excitation energy for central collisions only (610 MeV) is replaced by the full distribution. Solid line is experimental data.

overpredict $M = 1$ events by a factor of 2 and underpredict the largest multiplicities by up to a factor of 10. Thus, it appears that both the Δ resonance and source expansion are essential to account for the data in the context of the ISABEL/EES model. Although not shown, omission of both these effects underpredicts the data by orders of magnitude for $M = 4$. In order to obtain a satisfactory fit value of K larger than 144 in this model, the INC excitation energy distribution would have to be skewed to significantly higher values of E^* than shown in Fig. 3. While we have chosen INC input parameters and options that should optimize high excitation energies (notably fast rearrangement), the sensitivity of the energy dissipation to in-medium effects cannot be ignored. Thus, for example, if the probability for pion reabsorption, nucleon-nucleon, and/or Δ scattering in-medium are actually much larger than the input values, equivalent fits with larger values of K could be obtained.

The importance of employing a realistic distribution of excitation energies and source size in performing multifragmentation calculations is illustrated in Fig. 8. Here we have replaced the full distribution of excitation energy with the average value predicted by the INC code for the 3.6 GeV ^{3}He+^{nat}Ag reaction. Even with Δ formation and $K = 144$, the results are in strong disagreement with the data. This simply emphasizes the need for a full treatment of the initial excitation energy distribution as a starting point in order for calculations to be compared with data quantitatively.

In addition to the multiplicity distribution, we have also examined the predictions of differential spectral shapes obtained from the INC/EES models. We shall show below that these are in qualitative agreement with the spectra of IMFs observed in ^{3}He+^{nat}Ag.

First, we summarize the prominent features found in the data. In Fig. 9, which contains a selection from previously published data [27], it can be seen that the lower energy regions of the spectral peaks broaden as one goes to higher bombarding energy, and that there is also a qualitative change in the shape of the high-energy tails of the spectra. These changes are most abrupt between the incident energies of 0.90 and 1.8 GeV. It is in this bombarding energy range that the probability for excitation energies about $E^* \geq 500$ MeV becomes significant (Fig. 4).

To obtain a calculated prediction, we have used the EES model to generate a set of differential cross sections of fragments arising from the evolution of residues beginning from specific initial conditions, labeled by i, $d\sigma/d\Omega(E_i^*, A_i, Z_i, p_\parallel)$. Figure 9(b) gives a representative set of differential cross sections for carbon fragments taken at $E_i^* = 100$ to 900 MeV, in 200 MeV steps. For

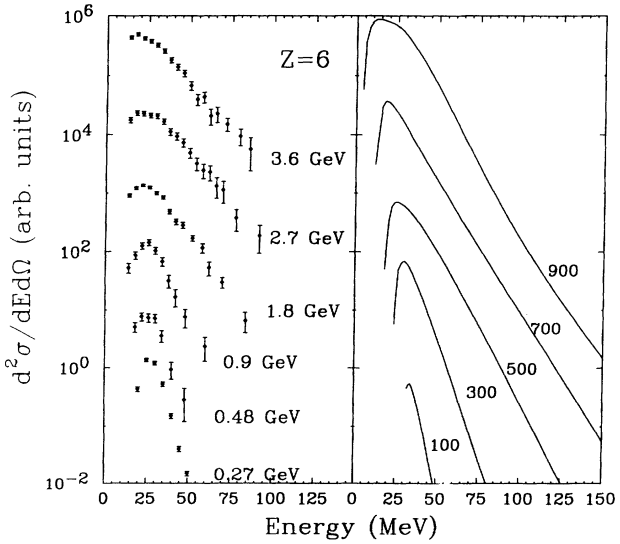

FIG. 9. Left frame: inclusive spectra for C fragments at backward angles for ^{3}He+^{nat}Ag reaction [27] as several bombarding energies. Right frame: Spectral shapes predicted by EES model for emission of $Z = 6$ fragments at 117° for several residue excitation energies (in MeV), as indicated on figure.

excitation below 400 MeV, the spectral shapes remain essentially the same with little change in the location or shape of the Coulomb peak. However, above this energy, the calculated Coulomb peaks broaden dramatically toward lower kinetic energies. This effect arises in the EES model as a consequence of fragment emission from a dilute system, which lowers the mutual Coulomb repulsion experienced by the emitted fragments. Similarly, the slope of the high-energy tails of the spectra become harder for $E^* \geq 500$ MeV. This behavior is a consequence of boosting the velocity of the emitted particles by the expansion velocity of the source.

The spectra of C fragments has previously been reported for selected events characterized by the value of the IMF multiplicity [8]. We review these data in Fig. 10, where the results show C fragments at laboratory angles of 35°, 63°, and 117° for events with IMF multiplicity $M = 1, 2, 3$. To compare the predictions of the model with these data, it is necessary to sum over the distribution of the sources produced in the initial phase of the reaction. This is indicated by the following sum

$$d\sigma/d\Omega_M = \sum_i \Delta E^* W(i) P(M; E_i^*, A_i, Z_i) \times d\sigma/d\Omega(E_i^*, A_i, Z_i, p_\parallel), \quad (3)$$

where M indicates the multiplicity of IMFs characterizing the cross section. No account has been made for the distribution in $p_\perp$, which would serve to broaden the calculated distributions further. The weights $W(i)$ were obtained from the INC, and the other factors were obtained from the EES model. The application of Eq. (3) to the case of the 3.6 GeV incident ^{3}He, provides the result displayed in Fig. 10 for carbon fragments. For comparison with the data, the respective curves are scaled by the M-dependent efficiencies suggested in Ref. [8]. In general, the calculated Coulomb peaks are higher and the spectral slopes are steeper than the data.

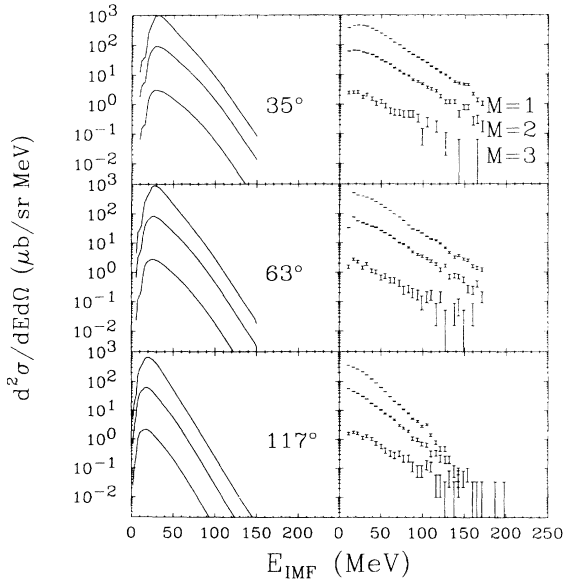

FIG. 10. Right frame: Data from Ref. [8] for carbon spectra at angles of 35° (top), 63° (middle), and 117° (bottom). In each case, the multiplicity of IMFs is identical to that indicated in upper frame. Left frame: INC/EES calculations for same spectra as in left frame.

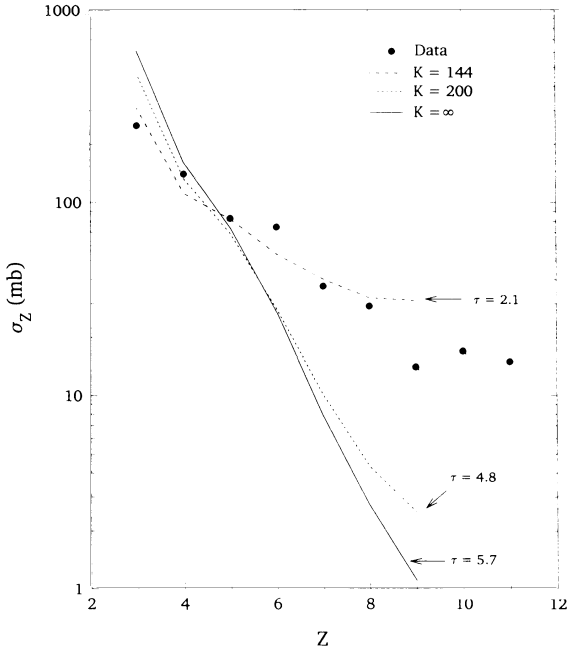

FIG. 11. Experimental inclusive charge distribution for 3.6 GeV ^{3}He+^{nat}Ag reaction (points) compared with predictions of INC/EES model for $K = 144$, $K = 200$, and $K = \infty$.

In order to provide a better fit to the spectra with the INC/EES model, several modifications merit consideration. Among these are (1) an increase in the Δ cross section in medium, which would extend the excitation energy distribution to higher energies; (2) inclusion of INC-generated fluctuations by using distributions other than average values, and (3) adding an additional expansion velocity from the INC stage of the reaction. Nonetheless, in qualitative terms, the INC/EES model provides a consistent description of the energy spectra, and the models suggest transparent explanations for the change in the gross features with increasing energy.

It is also of interest to compare the charge distributions predicted by the INC/EES model with the experimental data. In Fig. 11, we present such a comparison with a calculation which employs the standard (with Δ) INC code with the EES model for various values of the effective compressibility parameter K. The calculation is quite sensitive to the value of K; a value of $K = 144$ for the INC/EES model again gives the best fit to the data. Thus the results for the charge distributions are self-consistent with other observables.

IV. SUMMARY

In summary, multifragment emission data from the ^{3}He+Ag reaction have been examined in the framework

of a hybrid model that treats the reaction dynamics in terms of an intranuclear cascade calculation, followed by decay from an expanding, emitting source.

The INC calculations demonstrate that the average excitation of the excited residues formed in central collisions increases rapidly with bombarding energy; for more peripheral collisions this increase is much more gradual. The important role of the Δ resonance in producing highly excited residues is illustrated by the calculations. This mechanism provides a rapid, efficient means of energy dissipation that is necessary to form the highly excited species required for multifragmentation in light-ion-induced reactions. It also significantly accelerates the equilibration process [33]. The results suggest that multifragmentation studies, when complemented by pion emission probabilities, may provide valuable insight into the question of pion production and reabsorption in the nuclear medium. The INC calculations also show that $p_{\|}$ and $p_{\perp}$ are comparable for excitation energies in the vicinity of 600–700 MeV; for lower E^* values, $p_{\perp}$ is large, while for higher values, $p_{\|}$ is the larger component. These calculated values are consistent with source velocities derived from a rapidity analysis of the spectra for high multiplicity events in the ^{3}He+Ag system.

Fits to the 3.6 GeV ^{3}He+Ag data with the combined INC/EES model and $K = 144$ describe the multiplicity and charge distribution data best. Calculations with stiffer equations of state or without Δ excitations in the cascade severely underpredict the high multiplicity data; in fact,the calculations are quite sensitive to all parameters. In order to describe the data with a stiffer equation of state, the probability for Δ excitation and/or pion absorption in the INC code would need to be increased significantly in order to enhance the probability for high excitation energy residues.

The importance of employing a realistic excitation energy distribution in multifragmentation calculations is also stressed by this work. If the EES calculations are performed with the average INC excitation energy instead of the full distribution, the data are significantly underpredicted. Comparison of the INC/EES calculations with experimental kinetic energy spectra accounts for the major features of the data. The calculations successfully predict changes in IMF spectral shapes for ^{3}He bombarding energies below and above about 1 GeV, i.e., broadening of the Coulomb peaks toward lower energies and flattening of the spectral tails at high projectile energies, as observed in the data [27]. In the context of the EES model, this behavior is explained in terms of energetic IMFs being emitted early in the expansion, where the expansion velocity is large, and low energy IMFs being emitted from nuclear matter at low density. While the quantitative agreement with the spectra is not perfect the qualitative features of the data are successfully described.

In conclusion, these INC-EES calculations provide a physically transparent framework for understanding the basic features of light-ion-induced multifragmentation reactions. The fundamental roles of inealstic N-N scattering and expansion of the nuclear medium are essential in confrontation of this model with the data.

ACKNOWLEDGMENTS

The authors thank Zev Fraenkel for providing us with the ISABEL INC code. This work was supported by the U.S. Department of Energy, the National Science Foundation, and CEN Saclay.

[1] W. A. Friedman, Phys. Rev. **42**, 667 (1990).
[2] B. Li, W. Bauer,and G. Bertsch, Phys. Rev. C **44**, 2095 (1991).
[3] D. H. E. Gross, Nucl. Phys. **A553**, 175c (1993).
[4] J. Cugnon and C. Volant, Z. Phys. A **334**, 435 (1989).
[5] M. Begemann-Blaich *et al.*, Phys. Rev. C **45**, 677 (1992).
[6] D. R. Bowman *et al.*, Phys. Rev. Lett. **67**, 1527 (1991); Phys. Rev. C **46**, 1834 (1992).
[7] C. A. Ogilvie *et al.*, Phys. Rev. Lett. **67**, 1214 (1991).
[8] S. J. Yennello *et al.*, Phys. Rev. Lett. **67**, 671 (1991).
[9] K. Hagel *et al.*, Phys. Rev. Lett. **68**, 2141 (1992).
[10] V. E. Viola, Nucl. Phys. **A502**, 531c (1989); **471**, 53c (1987).
[11] F. Saint-Laurent, M. Conjeaud, R. Dayras, S. Harar, H. Oeschler, and C. Volant, Nucl. Phys. **A422**, 307 (1984).
[12] W. Loveland, K. Aleklett, L. Sihver, Z. Xu, C. Casey, D. J. Morrissey, J. O. Liljenzin, M. de Saint-Simon, and G. T. Seaborg, Phys. Rev. C **41**, 973 (1989).
[13] Y. Yariv and Z. Fraenkel, Phys. Rev. C **20**, 2227 (1979); **24**, 488 (1981).
[14] J. Cugnon, T. Mizutani, and J. Vandermeulen, Nucl. Phys. **A352**, 505 (1981).
[15] G. Bertsch and Das Gupta, Phys. Rep. **160**, 189 (1988).
[16] J. Aichelin, G. Peilert, A. Bohnet, A. Rosenhauer, H. Stöcker, and W. Greiner, Phys. Rev. C **37**, 2451 (1988).
[17] C. Gregoire, D. Jacquet, M. Pi, B. Remaud, F. Sebille, E. Suraud, P. Schuck, and L. Vinet, Nucl. Phys. **A471**, 399c (1987).
[18] D. H. E. Gross, L. Satpathy, M. Ta-chung, and M. Satpathy, Z. Phys. A **309**, 41 (1982).
[19] H. W. Barz, J. P. Bondorf, R. Donangelo, I. N. Mishustin, and H. Schulz, Nucl. Phys. **A448**, 753 (1986); J. P. Bondort *et al.*, *ibid.* **A444**, 460 (1985).
[20] R. Charity *et al.*, Nucl. Phys. **A483**, 371 (1988).
[21] W. Bauer, U. Post, D. R. Dean, and U. Mosel, Nucl. Phys. **A452**, 699 (1986).
[22] J. Aichelin, J. Hüfner, and R. Ibarra, Phys. Rev. C **30**, 107 (1984).
[23] J. Randrup and S. E. Koonin, Nucl. Phys. **A471**, 3552 (1987).
[24] T. S. Biro, J. Knoll, and J. Richert, Nucl. Phys. **A459**, 692 (1986).
[25] C. Ngô, Nucl. Phys. **A488**, 233c (1988).
[26] W. G. Lynch, Annu. Rev. Nucl. Sci. **37**, 493 (1987).

[27] S. J. Yennello *et al.*, Phys. Lett. B **246**, 26 (1990).
[28] A. Y. Abdul-Magd, W. A. Friedman, and J. Hüfner, Phys. Rev. C **34**, 113 (1986).
[29] J. Cugnon, Nucl. Phys. **A462**, 751 (1987).
[30] M. L. Clover, R. M. DeVries, N. J. DiGiacomo, and Y. Yariv, Phys. Rev. C **26**, 2138 (1982).
[31] S. J. Yennello *et al.*, Phys. Rev. C **48**, 1092 (1993).
[32] J. Cugnon and M. C. Lemaire, Nucl. Phys. **A489**, 781 (1988); M. C. Lemaire *et al.*, in *Proceedings of the International Workshop on Gross Properties of Nuclei and Nuclear Excitations XIX*, Hirschegg, edited by H. Feldmeier (GSI Report ISSN 0720-8715, 1991), p. 73.
[33] M. Cubero, M. Schönhofen, B. L. Friman, and W. Nörenberg, Nucl. Phys. **A519**, 345c (1990).